International Journal of Mechanical Engineering and Applications
2024; 12(1): 8-17
http://www.sciencepublishinggroup.com/j/ijmea
doi: 10.11648/j.ijmea.20241201.12
ISSN: 2330-023X (Print); ISSN: 2330-0248 (Online)

Mechanical Properties of Spherical Deep-Sea Pressure Structures by Integral Hydrobulge Forming with Triangular Patch Polyhedrons

Yang Jing[1], Chenghai Kong[2], Jingchao Guan[1, *], Wei Zhao[3], Xilu Zhao[1]

[1]Department of Mechanical Engineering, Graduate School, Saitama Institute of Technology, Saitama, Japan

[2]Topy Industries Co., Ltd., Aichi, Japan

[3]National Institute of Technology, Toyama College, Toyama, Japan

Email address:

keiyou1012@gmail.com (Yang Jing), kongchenghai@gmail.com (Chenghai Kong), guanjingchao123@gmail.com (Jingchao Guan), shunsuke0390@gmail.com (Wei Zhao), zhaoxilu@sit.ac.jp (Xilu Zhao)

[*]Corresponding author

To cite this article:

Yang Jing, Chenghai Kong, Jingchao Guan, Wei Zhao, Xilu Zhao. (2024). Mechanical Properties of Spherical Deep-Sea Pressure Structures by Integral Hydrobulge Forming with Triangular Patch Polyhedrons. *International Journal of Mechanical Engineering and Applications*, *12*(1), 8-17. https://doi.org/10.11648/j.ijmea.20241201.12

Received: December 14, 2023; **Accepted**: January 2, 2024; **Published**: January 23, 2024

Abstract: Manned pressure shells subjected to deep-sea pressure are designed with a spherical shell structure because they are subjected to perfectly symmetrical pressures. A spherical pressure shell has excellent mechanical properties against deep-sea pressure; therefore, it has the advantage of relatively good buckling properties. However, there are high demands on the processing accuracy of spherical pressure shells, such as thickness distribution and roundness. Even when a small asymmetrical element is present, the buckling characteristics under deep-sea pressure are significantly reduced. In this paper, we propose a new type of spherical pressure shell composed of multiple triangular-plate parts and an integral hydrobulging forming (IHBF) method to process it. Specifically, multiple triangular metal plate parts were prepared and welded along the right side to form a preformed box. A spherical pressure shell was plastically formed by applying water pressure to the interior of the preformed box, causing it to expand outward. For verification, an actual molding experiment was conducted using a spherical pressure shell with a design radius of 250 mm as the research object. The measurement of the outer surface shape of the formed spherical pressure shell showed that the radius value of the spherical pressure shell was 246.52 mm, the error from the design radius was 1.39%, the roundness of the spherical surface was 3.81 mm, and the maximum reduction rate of the plate thickness was 3.2%. Therefore, the processing quality of the proposed IHBF method was confirmed to be high. Buckling analysis was performed by applying a uniformly distributed external pressure to simulate the deep-sea pressure. Compared with the conventional spherical shell structure, the crushing/buckling load of the spherical pressure shell processed by the IHBF method proposed herein is affected by work hardening owing to plastic forming, local defects, and welding line. The effect of the size is relatively small.

Keywords: Spherical Deep-Sea Pressure Hull, Spherical Shell Pressure Properties, Integral Hydrobulging Forming, Spherical Pressure Vessel, Plastic Forming Method

1. Introduction

The pressure hulls used in the deep sea are subjected to a perfectly symmetrical water pressure. As it is most rational to apply a symmetrical structure to symmetrical loading conditions, all deep-sea pressure shells are spherical [1-5].

Considering the loading conditions of spherical pressure hulls used in the deep sea, studies have been published on the crushing/buckling characteristics of spherical shell structures subjected to uniformly distributed compressive loads from the outside [6-11]. In addition to theoretical studies, including linear and nonlinear considerations, the finite element method (FEM) has been used to conduct detailed studies on the crushing/buckling characteristics of spherical pressure hulls [12-13]. These results have become a useful basis for the

design and development of spherical pressure hulls, assuming the approximation of a perfect spherical shell structure.

Actual manned spherical pressure hulls have entrances, observation windows, etc.; therefore, they do not satisfy perfect symmetry conditions. Therefore, studies have been conducted on the effects of local defects and geometric asymmetry on the crushing/buckling characteristics of spherical pressure hulls [14-17]. To overcome these problems, studies have been conducted to adjust the wall thickness distribution of a spherical pressure hull to improve its crushing/buckling characteristics; however, the problem has not been solved [18-20].

However, the shape accuracy of a spherical pressure hull in an environment exposed to high deep-sea pressures has a significant influence on its crushing characteristics. Therefore, the processing quality of a spherical pressure-resistant hull must be improved, and this processing problem has become an important issue.

The conventional processing method involves heat-pressing the plate materials to form curved parts and then assembling a spherical pressure hull by welding [21-22]. Integral hydrobulging forming (IHBF) was proposed to improve the processing shape accuracy and solve uneven thickness problems. When utilizing the IHBF method, water pressure is applied inside the preformed box welded from the flat-plate parts to expand the preformed box into a spherical hull structure [23-25]. Using a preforming box as close to a spherical shape as possible and with a perfectly symmetrical water pressure acting inside, the wall material distribution of the expansion-molded spherical hull structure has the advantage of being relatively uniform [26-28].

The machining accuracy and quality of a spherical pressure hull can be improved by applying the IHBF method. However, it is necessary to continue investigating whether mechanical properties, such as the crushing/buckling load, of a spherical pressure hull fabricated using the IHBF method can be applied to deep-sea pressure environments.

In this study, to improve the machining quality and crushing/buckling characteristics of deep-sea spherical pressure hulls formed using IHBF, a new type of spherical pressure hull was devised and an IHBF method consisting of triangular flat-plate parts to be processed was proposed. The design formula for the dimensions of the triangular-plate parts and the calculation formula for the water pressure required for IHBF were derived. For confirmation, the stress and plate thickness distributions of the simulated IHBF process were analyzed using the FEM. An IHBF plastic-forming experiment was conducted using a design radius of 250 mm as the target. The average radius and surface roundness of the IHBF-formed spherical pressure hull were measured using a laser measuring device to verify the forming quality of the spherical pressure hull processed using the IHBF method. Furthermore, an FEM analysis was performed by applying a uniformly distributed pressure to the molded spherical pressure hull. A detailed study was performed on the effects of work hardening, local defects, and weld lines on the crushing/buckling characteristics.

2. Materials and Methods

2.1. IHBF Forming Methods

The IHBF method, shown in Figure 1, was proposed to process spherical tanks with high shape accuracy and quality. As shown in Figure 1, this method involves (a) cutting the flat part, (b) bending it, (c) welding it into the closed preform box, and (d) applying water pressure inside it so that the spherical pressure hull can be processed [24].

However, when processing a spherical pressure hull using the IHBF method, it is necessary to weld the flat-plate parts to form a preformed box structure before performing bulge forming using the internal water pressure. The preformed box structure must be as spherical and symmetrical as possible. Therefore, an IHBF processing method using a ball-shaped preforming box, as shown in Figure 2, was proposed and studied [26]. Furthermore, to reduce the amount of plastic deformation during IHBF processing and obtain a more uniform plate thickness distribution, a preformed box consisting of triangular patches obtained from a soccer-ball shape was devised [28].

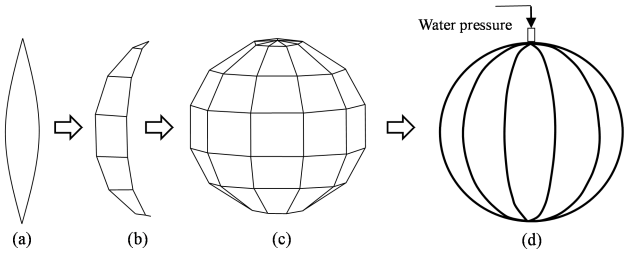

Figure 1. *Spherical tank manufacturing using the proposed IHBF method [24].*

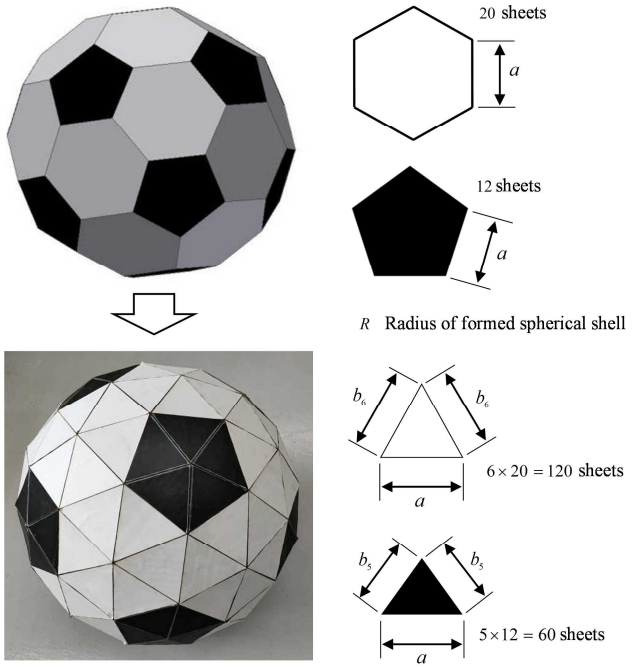

Figure 2. *Soccer-ball-type and triangle-type preformed boxes using the IHBF method [26, 28].*

Figure 2 Soccer-ball-type and triangle-type preformed boxes using the IHBF method [26, 28]

As shown in Figure 2, if the radius of the spherical shell formed by the IHBF method is R, the side lengths, a, of the regular hexagon and pentagon of the soccer-ball-shaped preforming box can be calculated using the following formula [26]:

$$a = 0.40353R \tag{1}$$

Furthermore, each regular hexagon and pentagon was divided into triangles. The side length b6 of an isosceles triangle divided by a regular hexagon and the side length b5 of an isosceles triangle divided by a regular pentagon were calculated using the following formulas [28]:

$$b_6 = 0.41241R \tag{2}$$

$$b_5 = 0.34862R \tag{3}$$

To fabricate the soccer-ball-shaped preforming box, 20 regular hexagonal and 12 regular pentagonal flat-plate parts were required. To fabricate the triangular-patch preform box, 120 regular hexagonal triangles and 60 regular pentagonal triangular plates were required.

In this study, a spherical pressure hull forming experiment was conducted using the IHBF method using a triangular-patch-type preformed box to obtain a plate thickness distribution that minimized the amount of plastic deformation and made it more uniform.

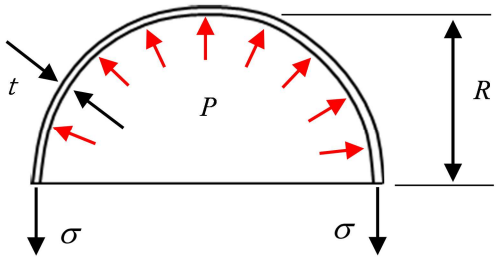

Figure 3. *Calculation of internal water pressure required for IHBF.*

To calculate the water pressure required for the forming process, the spherical pressure shell was cut in half and analyzed, as shown in Figure 3. The relationship between the internal water pressure P and the sidewall stress during plastic forming can be calculated using the following formula:

$$\sigma = \frac{PR}{2t} \tag{4}$$

where t denotes the thickness. During plastic forming, when the stress acting on the sidewall of the spherical pressure hull reached the yield stress, plastic deformation began. The required water pressure was calculated using the following equation:

$$P = \frac{2t\sigma_s}{R} \tag{5}$$

2.2. Forming Process of Spherical Pressure Hull

Based on the results in the previous section, an IHBF experiment was conducted on a spherical pressure shell using a triangular preforming box. The material used was stainless steel SUS304, and the plate thickness was 1.0 mm. A spherical pressure hull with a radius R = 250 mm was used in the forming experiment.

The side lengths of the two types of isosceles-triangular-plate parts were calculated using design formulas (1), (2), and (3). The base length of the isosceles triangle was a = 100 mm, the equilateral length of the isosceles triangle obtained from the regular hexagon was b6 = 102 mm, and the equilateral length of the isosceles triangle plate b5 obtained from the regular pentagon was 86 mm.

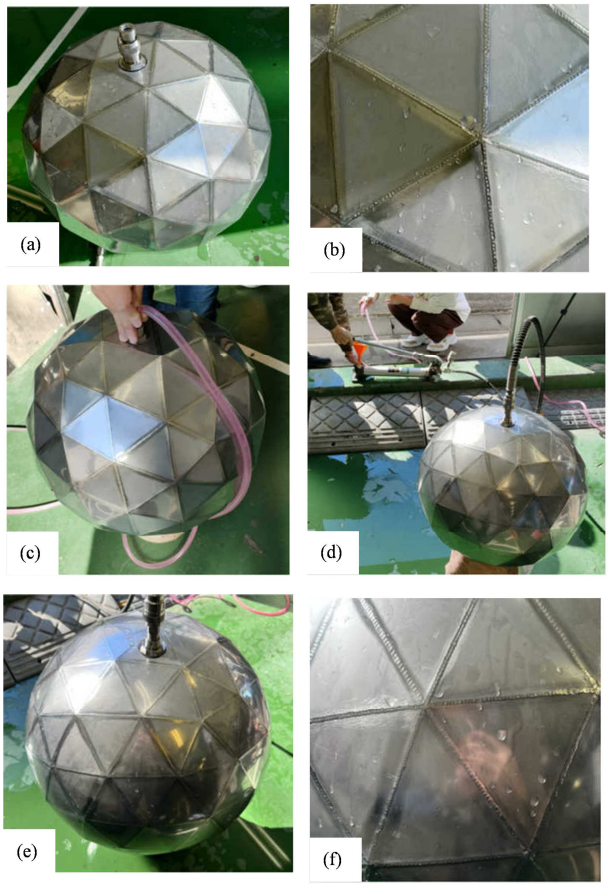

Figure 4. *Manufacturing process of a spherical pressure hull using the IHBF method.*

The plastic forming process is shown in Figure 4. As shown in Figure 4(a), 120 regular hexagonal triangles and 60 regular pentagonal triangles were cut using a laser processing machine, and each flat-plate part was welded to a triangular preform box. A bulkhead socket was attached to the center of one of the triangular plates. Figure 4(b) shows the welded local area.

As shown in Figure 4(c), water was injected into the interior of the triangular preforming box to the fullest extent through the bulkhead socket.

Subsequently, as shown in Figure 4(d), water pressure was applied to the inside of the preforming box using a manual hydraulic pump to perform the plastic forming of the preforming box so that it expanded.

Consequently, the water pressure could be maintained until

the preformed box had a round spherical shape, as shown in Figure 4(e). Finally, the water in the formed spherical pressure hull was drained to complete the plastic forming process. The local area is shown in Figure 4(f).

Figure 4 shows that the spherical pressure hull formed using the IHBF method was processed into a spherical shape.

3. Results

The shape accuracy of the plastically formed spherical pressure hull was quantitatively confirmed. As shown in Figure 5, the shape data of the spherical pressure shell was measured using a camera stand, rotary table, and laser displacement meter (CD22-35VM12 manufactured by OPTEX, measurement accuracy ±0.01 mm). In Figure 5, the coordinate transformation was performed by measuring the height from the camera stand, the distance from the laser displacement meter, and the angle from the rotary table. Consequently, three-dimensional coordinate values of the surface of the spherical pressure shell could be obtained.

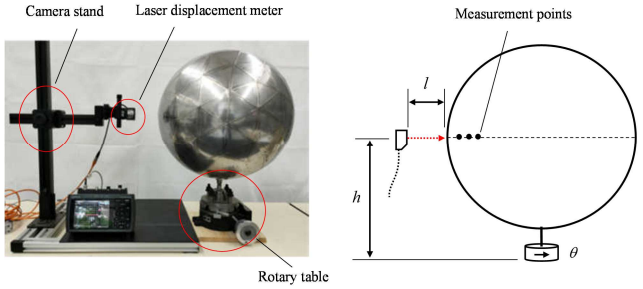

Figure 5. *Surface shape data measurement for the formed spherical pressure hull.*

For the measurement, the height of the camera stand was adjusted to the position where the distance read from the laser displacement meter was the greatest, and the height h and distance l were recorded. The rotary table was then rotated every 5°, and each measurement was recorded.

Figure 6 shows the results of the actual measurements taken at the sample points on the surface of the central cross-section of the spherical pressure shell. The solid blue line represents the true circle, and the red dotted line represents the position of the measurement sample point. The dimensional accuracy of the plastic-formed spherical pressure hull was investigated, and the measured value of the radius of the central cross-section was 246.52 mm, which was an error of 1.39% compared with the design value of 250 mm. It was verified that design formulas (1)–(3) of the triangular flat-plate parts for forming spherical shells were correct.

The shape accuracy of the formed spherical pressure hull was also investigated. The maximum distance from the center point to the measurement sample point was 248.28 mm, and the minimum distance was 244.47 mm. Therefore, the obtained roundness was 3.81 mm. The shape accuracy of the formed spherical pressure hull was satisfactory.

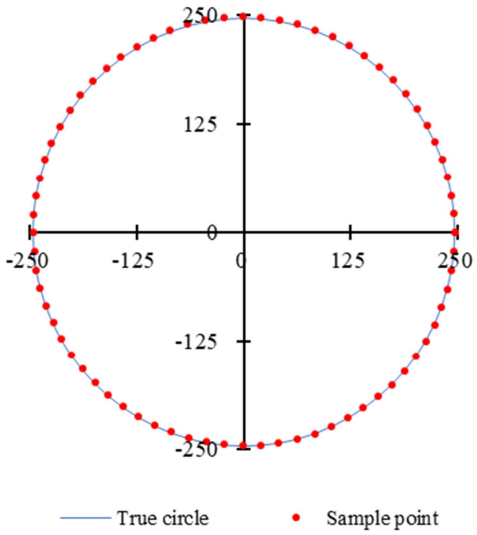

Figure 6. *Measurement results of the formed spherical pressure hull.*

4. Discussion

The results section should provide an accurate and concise description of the experimental findings, and the resulting conclusions that can be inferred from the experiments. Meanwhile, the results should be presented in a transparent and truthful manner, avoiding any fabrication or improper manipulation of data. Where applicable, results of statistical analysis should be included in the text or as tables and figures.

4.1. Forming Analysis of Spherical Pressure Hull

When using the measurement system shown in Figure 5, it is not possible to obtain detailed data, such as the stress during the plastic forming of a spherical pressure hull and the distribution of the plastically formed wall thickness.

In this study, we used the FEM to analyze the plastic forming process of a spherical pressure hull. The FEM analysis model is shown in Figure 7 using quadrilateral and triangular elements, and the average side length of the elements was 5 mm. The plate thickness was set as 1 mm. The Young's modulus of the stainless-steel SUS304 material was 193 GPa, and the Poisson's ratio was 0.3. Figure 8 shows the stress–strain relationship used for the plastic deformation, where the yield stress was 205 MPa. Based on the results of the plastic forming experiments, the maximum internal water pressure for forming was set to 2.3 MPa.

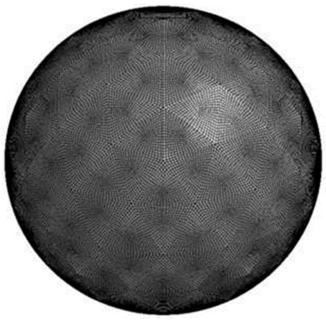

Figure 7. *FEM analysis model.*

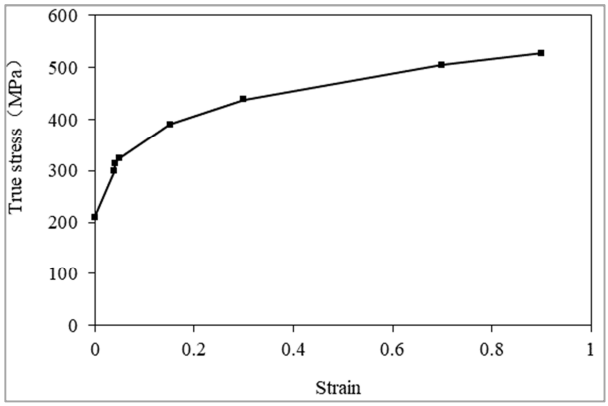

Figure 8. *Stress–strain relationship graph.*

Figures 9 and 10 show the results of the analysis of the von Mises stress and plate thickness distributions upon the completion of plastic forming, respectively. The figure shows that the IHBF plastic forming develops uniformly and forms a smooth spherical pressure hull surface because the internal water pressure is perfectly symmetrical.

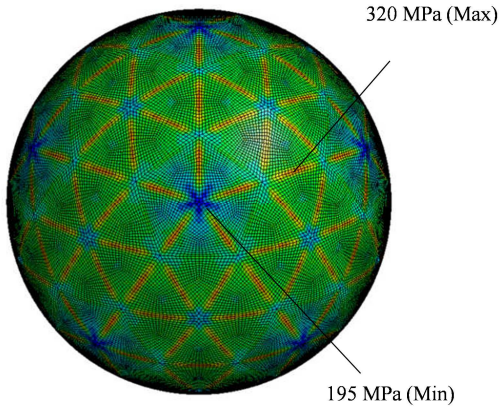

Figure 9. *Von Mises stress distribution.*

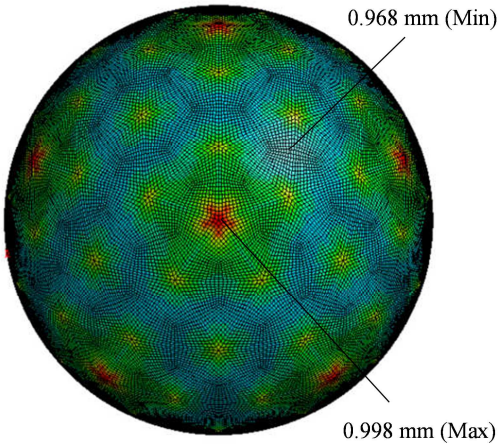

Figure 10. *Thickness distribution.*

According to the stress distribution results shown in Figure 9, the maximum stress was distributed along the weld line, which was believed to be caused by the bending stress experienced by the folded weld line. The minimum stress occurred at the center point of the original regular pentagon. The maximum von Mises stress value was 320 MPa, and the minimum von Mises stress value was 195 MPa.

The plate thickness distribution results shown in Figure 10 indicate that the plate tended to be slightly thinner overall compared with the plate of thickness 1.0 mm before forming. The thinnest plate was 0.968 mm, with a thickness reduction rate of 3.2%. The thickness of the plate with the smallest reduction was 0.998 mm, with a plate thickness reduction rate of 0.20%.

4.2. Effect of Work Hardening on Crushing/Buckling Load

When a metal is used to develop a deep-sea pressure hull, it is necessary to consider its work hardening effect caused by plastic forming to apply a uniformly distributed load to the formed spherical pressure hull and evaluate the crushing/buckling strength accurately.

For comparison, two cases were analyzed for the same analytical model of a spherical pressure hull: one in which work hardening was considered and one in which work hardening was not considered. The results of this analysis are shown in Figure 11. The horizontal axis represents the external pressure, and the vertical axis represents the maximum von Mises stress. The red line represents the results considering work hardening, the black line represents the results not considering work hardening, and the blue dotted line represents the results for a simple spherical shell structure.

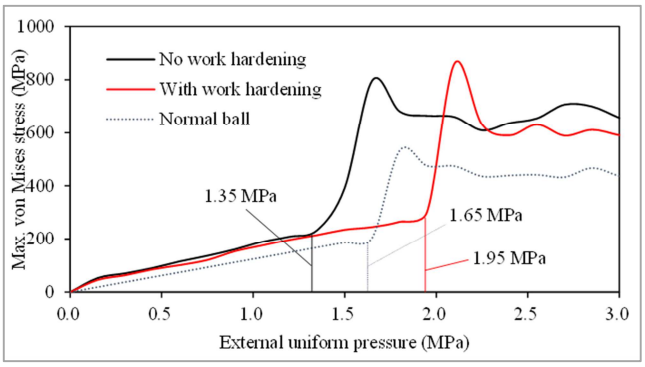

Figure 11. *Results of crush deformation analysis with and without the consideration of work hardening.*

As shown in Figure 11, at the initial stage of application of external pressure, there is a linear relationship between the pressure and the stress; however, when the external pressure reaches a certain value, the stress suddenly increases. This indicates the occurrence of crushing/buckling.

The crushing/buckling load of the spherical pressure hull without considering work hardening is 1.35 MPa, which is lower than the crushing/buckling load of the simple spherical hull structure, which is 1.65 MPa. However, after considering the work hardening after plastic forming, the crushing/buckling load of the spherical pressure hull is 1.95 MPa, indicating that it has a higher crushing/buckling load than a simple spherical shell structure.

Figure 12 shows the crushing/buckling modes for each analysis case. Figure 12 shows that work hardening has a

greater effect on the crushing/buckling load but has little effect on the crushing/buckling mode shape.

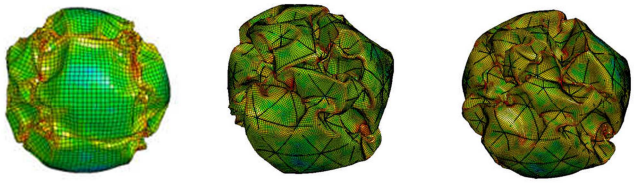

Figure 12. *Crush deformation mode with and without the consideration of work hardening.*

4.3. Effect of Local Defects on Crushing/Buckling Load

Even minute defects on the surface of a spherical pressure hull used for deep-sea pressure have a significant effect on the crushing/buckling load. For the analysis model shown in Figure 13, the plate thickness in an area with an equivalent diameter of 20 mm was reduced by half from 1.0 mm to 0.5 mm, and a collapse analysis of a spherical pressure hull was performed to simulate local defects.

For comparison, we set the following four analysis cases: (1) a spherical shell with no defects, (2) a spherical shell with defects, (3) a plastic-formed spherical pressure hull without defects, and (4) There is a defect in the spherical pressure hull and the center of the triangle.

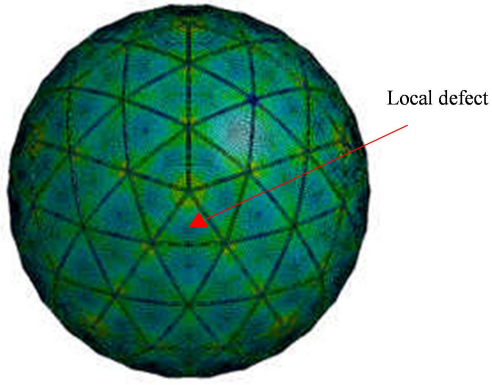

Figure 13. *Collapse analysis model with localized defects.*

The results of this analysis are shown in Figure 14. The solid black line represents the result of a simple spherical shell without a defect, and the black dotted line represents the result of a simple spherical shell with a defect. The solid red line represents the result of the formed spherical pressure hull without defects, and the red dotted line represents the result of the formed spherical pressure hull with defects.

According to Figure 14, the crushing/buckling load of a simple spherical shell without defects was 1.65 MPa. When there was a defect, the crushing/buckling load was reduced by 27.8% to 1.20 MPa owing to the concentration of crushing deformation on the local defect. By contrast, the crushing/buckling load of the spherical pressure hull formed without local defects was 1.95 MPa. The crushing/buckling load in the case with defects was 1.65 MPa, which is 18.2% lower than that in the case without defects.

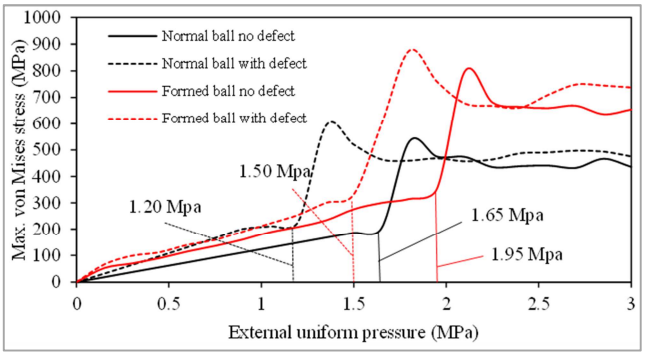

Figure 14. *Crush analysis results with and without the consideration of a local defect.*

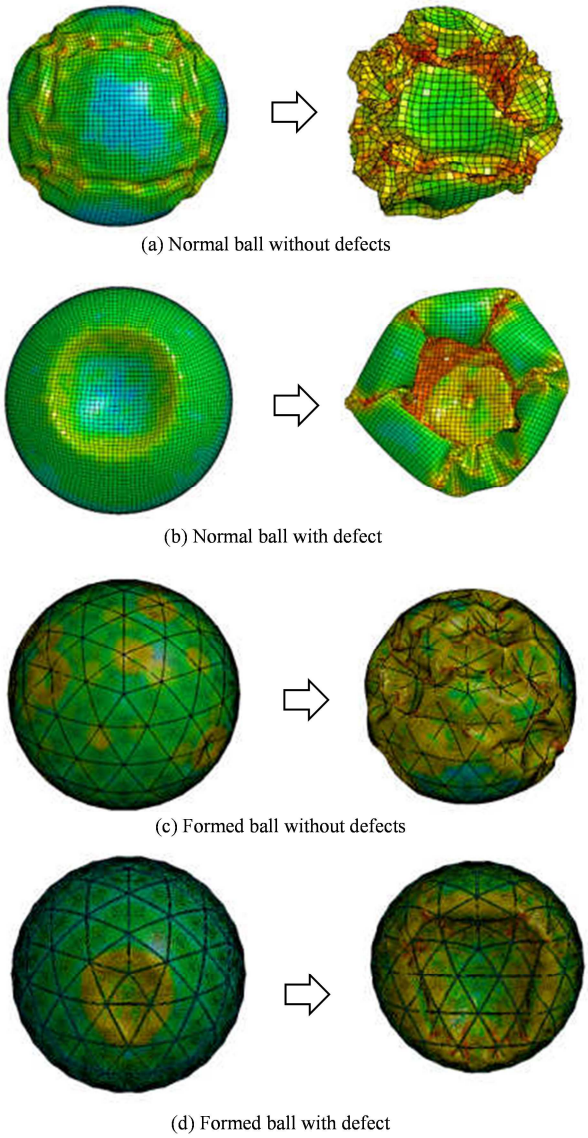

Figure 15. *Crushing/buckling modes with and without the consideration of a local defect.*

Figure 15 shows a comparison of the results of the crushing/buckling modes for each case. In the absence of local defects, crushing/buckling modes occur uniformly on a spherical surface. When a local defect exists, the crushing/buckling mode appears to originate from the defect

and gradually expands. It appears more advantageous to distribute the external pressure over the entire surface of the spherical structure than to concentrate it on a localized defect. Therefore, as shown in Figure 14, all the crushing/buckling loads were reduced owing to the presence of local defects.

Even if a similar local defect exists, it is relatively easy to unfold after crushing and buckling if there is a local defect on the surface of a simple spherical shell. If there are local defects on the surface of a plastically formed spherical pressure hull, expansion tends to be relatively difficult owing to the influence of the weld line.

4.4. Effect of Weld Line Width on Crushing/Buckling Load

A spherical pressure hull formed using IHBF always leaves the weld line; therefore, particularly with IHBF, it is necessary to examine the effect of the size of the weld line on the crushing/buckling load of the spherical pressure hull.

The influence of the welding line was considered, as shown in the crushing analysis model in Figure 16. The size of the beam element added along the welding line (diameter of the simplified circular cross section) was set to four analysis cases: 2.0 mm, 3.0 mm, 4.0 mm, and 5.0 mm. Each analysis was performed, and the results are shown in Figure 17.

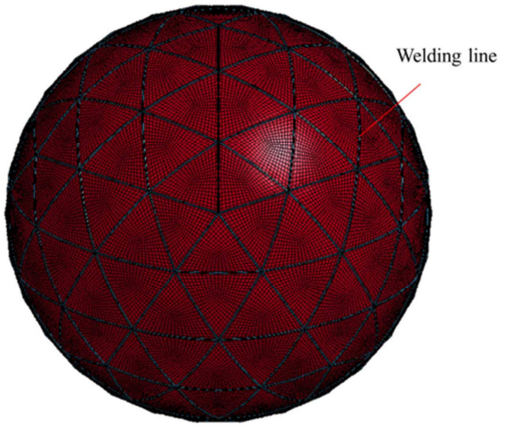

Figure 16. *Crush analysis model considering the effect of welding lines.*

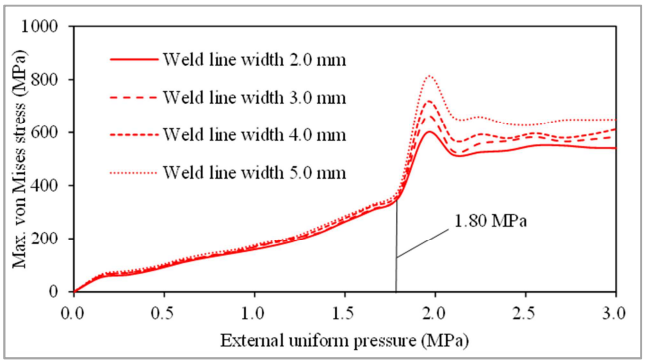

Figure 17. *Crush analysis results of the different welding lines.*

Figure 17 shows that, even when the welding line width was changed, the crushing/buckling load remained almost unchanged at 1.80 MPa. Therefore, the uniform distribution of the weld line was dominant in determining the crushing/buckling mode, and the influence of the weld line size on the crushing/buckling load was small.

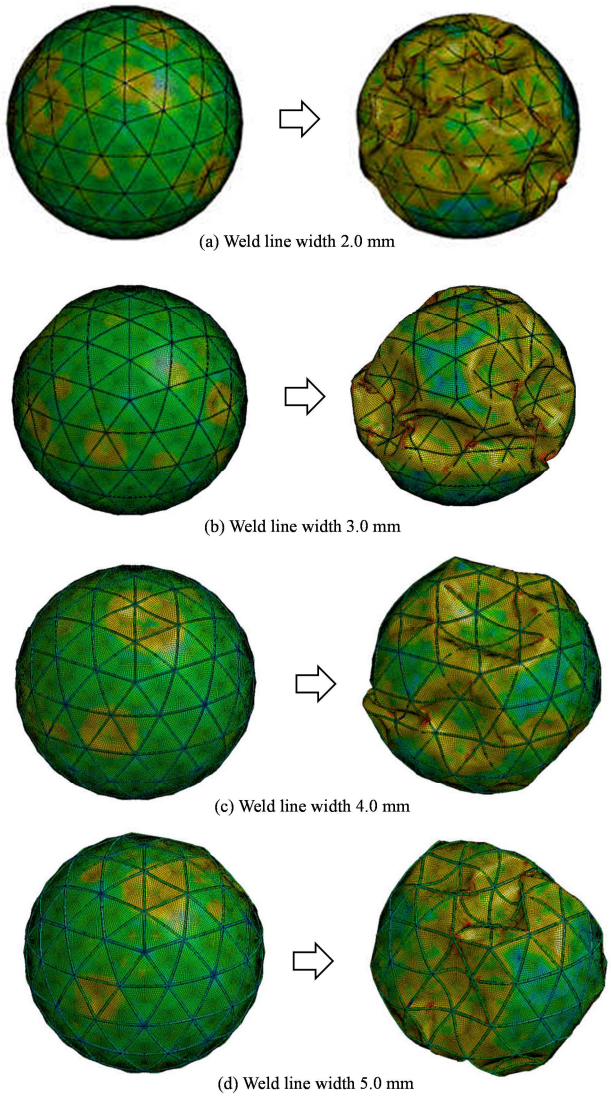

Figure 18. *Crushing/buckling mode results of the different welding lines.*

Figure 18 shows the crushing/buckling modes for each welding line. Figure 18 shows that the influence of the weld line width on the crushing/buckling mode was small.

4.5. Effect of Crushing/Buckling Mode Shape

As shown in Figure 19, two types of crushing/buckling modes exist for a spherical pressure hull. Figure 19(a) shows a pattern in which the crushing deformation was concentrated at one point, and Figure 19(b) shows a pattern in which the crushing deformation was uniformly distributed. From a mechanical perspective, it is more advantageous to improve the crushing/buckling performance if the crushing/buckling deformation is uniformly distributed along the outer shape of the spherical shell rather than being concentrated at one point.

In actual problems, if the structural shape of the spherical pressure hull and external load ideally have symmetry, the

crushing/buckling load will be high. In this case, the crushing/buckling mode exhibits a uniform distribution, as shown in Figure 19(b). This ideal crushing/buckling mode can be obtained through theoretical analysis. However, in actual structural problems, certain types of asymmetrical elements are induced, and a crushing/buckling mode concentrated at one point is commonly obtained, as shown in Figure 19(a). This results in a significant reduction in the crushing/buckling load. Therefore, to improve the crushing/buckling load of a spherical pressure hull structure, the crushing/buckling mode needs to be induced, to obtain a uniform distribution.

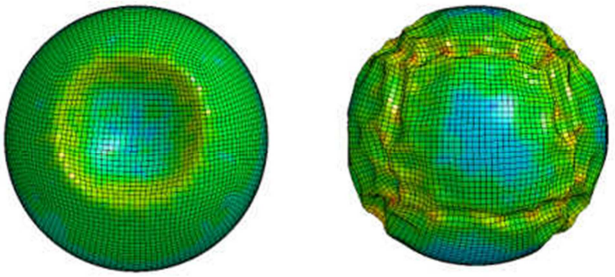

(a) Convergence crush mode (b) Uniformly distributed crushing mode

Figure 19. *Two crushing/buckling modes of a spherical shell structure under a uniform external load.*

In contrast, in the proposed triangular spherical pressure hull, the welding lines were uniformly distributed on the outer surface, as shown in Figure 20. The crushing/buckling mode exhibited a uniformly distributed deformation pattern, which is advantageous for improving the crushing/buckling load.

However, owing to the lack of perfect symmetry along the external shape, the crushing/buckling load tended to be lower than that of a simple spherical shell, as shown in Figure 20. However, as the wall material of the spherical pressure hull formed by bulge plastic forming owing to internal water pressure was work-hardened, the yield stress was high, and the crushing/buckling load was confirmed to be higher than that of a simple spherical shell.

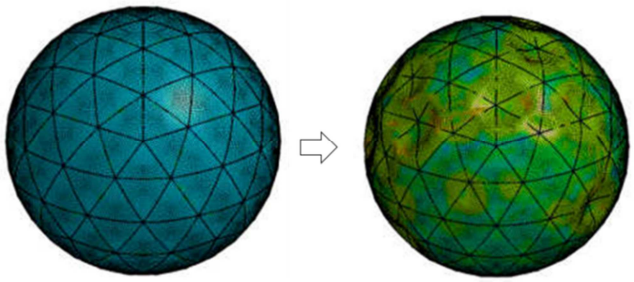

Figure 20. *Two crushing/buckling modes.*

In addition, the distribution positions of the triangular weld line uniformly distributed on the outer surface played an important role in forming the crushing/buckling mode of the spherical pressure hull. Therefore, the welding line became the dominant factor. Once the weld line was located, local defects and other factors, such as the width of the weld line, had a relatively small effect on the crushing/buckling load.

Therefore, compared with a simple spherical shell, a triangular spherical pressure hull has a higher crushing/buckling load owing to work-hardening and, simultaneously, variations, such as local defects, have a smaller influence on the crushing/buckling load. This characteristic can also be applied to deep-sea crewed pressure hulls.

5. Conclusions

In this study, a new triangular spherical pressure hull and an IHBF method for its fabrication were proposed to improve the design and manufacturing problems of spherical pressure hulls. A spherical pressure hull was plastically formed using the proposed IHBF method. A detailed study was conducted on the crushing/buckling performance of the resulting spherical pressure hull subjected to external hydraulic loads. The following conclusions were drawn.

(1) To realize the proposed IHBF plastic-forming process for a spherical pressure hull, a design formula for the dimensions of the triangular-plate parts and a practical calculation formula for the water pressure required for bulge forming were derived. We conducted a plastic forming experiment on a spherical pressure hull using a triangular preforming box and confirmed that the calculated formulas for the dimensions of the triangular flat-plate parts and forming water pressure were correct. Thus, the design problems necessary for processing the proposed spherical pressure hull were solved.

(2) IHBF plastic-forming experiments were conducted using a design target with a radius of 250 mm. The radius of the spherical pressure hull obtained via IHBF using the designed triangular-plate part was 246.52 mm, and the error from the design target radius was 1.39%. The surface of the spherical pressure hull was smooth, with a roundness of 3.81 mm. For verification, the plastic forming process was analyzed using the FEM; the maximum von Mises stress was 320 MPa, and the maximum reduction rate of the plate thickness was 3.20%. Therefore, it was verified that a spherical pressure hull could be stably formed using the proposed IHBF method and that the quality of the obtained spherical pressure hull was good.

(3) A crushing analysis was performed by applying an external pressure to verify the crushing/buckling performance of the spherical pressure shell plastic-formed using the IHBF method. Compared with the conventional simple spherical shell structure, the crushing/buckling load when the spherical pressure shell plastic-formed using the IHBF method underwent work hardening was 1.95 MPa, which is approximately 18.2% higher than that (1.65 MPa) of the simple spherical shell structure. It is believed that, by arranging uniformly distributed welding lines on the spherical pressure hull formed by IHBF, the resulting crushing/buckling mode is induced to have a uniform distribution.

(4) To verify the influence of the sizes of the local defects

and weld lines on the crushing/buckling performance of a plastically formed spherical pressure hull, an FEM analysis was performed by changing the setting conditions of the local defects and weld lines. The crushing/buckling load of a spherical pressure shell subjected to a symmetrically uniformly distributed pressure was significantly affected by local defects. The influence of the weld line size on the crushing/buckling load of the spherical pressure hull was relatively small.

(5) Although the spherical pressure hull has the advantages of good mechanical properties, However, the spherical pressure hull is a structure that is highly sensitive to defects. Therefore, further work should focus on how to reduce the impact of welding lines on the shape of the formed spherical shell, or conduct some discussions on practical application, i.e. making the experimental model into a real size.

ORCID

0000-0003-3668-7732 (Jingchao Guan)

Acknowledgments

We are grateful to all of those with whom we have had the pleasure to work during this and other related projects.

Conflicts of Interest

The authors declare no conflicts of interest.

References

[1] J. Zhang, X. ZUO, W. Wang, W. Tang, “Overviews of Investigation on Submersible Pressure Hulls,” Advances in Natural Science, 2014, Vol. 7(4), pp. 1–8. [CrossRef]

[2] W. Cui, “Development of the Jiaolong Deep Manned Submersible,” Marine Technology Society Journal, 2013, Vol. 47(3), pp. 37–54. [CrossRef]

[3] W. Cui, “An Overview of Submersible Research and Development in China,” Journal of Marine Science and Application, 2019, Vol. 17, pp. 459–470. [CrossRef]

[4] Y. Huang, K. Minami, M. Masuda, “A Design Method for Spherical Pressure Shells Subjected to External Pressure,” Transactions of Navigation, 2021, Vol. 6, No. 1, pp. 31–42. [CrossRef]

[5] A. Meschini, A. Ridolfi, J. Gelli, M. Pagliai, A. Rindi, “Pressure Hull Design Methods for Unmanned Underwater Vehicles,” Journal Marine Science and Engineering, 2019, Vol. 7, No. 382. [CrossRef]

[6] J. W. Hutchinson, “Buckling of spherical shells revisited,” Proceedings of the Royal Society A, 2016, Vol. 472, No. 20160577. [CrossRef]

[7] M. Imran, D. Shi, L. Tong, H. M. Waqas, R. Muhammad, M. Uddin, A. Khan, “Design Optimization and Non-Linear Buckling Analysis of Spherical Composite Submersible Pressure Hull,” Materials, 2020, Vol. 13, No. 2439. [CrossRef]

[8] J. Zhang, M. Zhang, W. Tang, W. Wang, M. Wang, “Buckling of spherical shells subjected to external pressure: A comparison of experimental and theoretical data,” Thin–Walled Structures, 2017, Vol. 111, pp. 58–64. [CrossRef]

[9] B. Pan, W. Cui, “An overview of buckling and ultimate strength of spherical pressure hull under external pressure,” Marine Structures, 2010, Vol. 23, pp. 227–240. [CrossRef]

[10] J. Zhang, M. Zhang, W. Cui, W. Tang, F. Wang, B. Pan, “Elastic-plastic buckling of deep sea spherical pressure hulls,” Marine Structures, 2018, Vol. 57, pp. 38–51. [CrossRef]

[11] B. Pan, W. Cui, Y. Shen, T. Liu, “Further study on the ultimate strength analysis of spherical pressure hulls,” Marine Structures, 2010, Vol. 23, pp. 444–461. [CrossRef]

[12] O. Adeyefa, O. Oluwole, “Finite Element Analysis of Von-Mises Stress Distribution in a Spherical Shell of Liquified Natural Gas (LNG) Pressure Vessels,” Engineering, 2011, Vol. 3, No. 10, pp. 1012–1017. [CrossRef]

[13] O. Adeyefa, O. Oluwole, “Finite Element Modeling of Shop Built Spherical Pressure Vessels,” Engineering, 2013, Vol. 5, No. 6, pp. 537–542. [CrossRef]

[14] H. Wagner, C. Hühne, J. Zhang, W. Tang, R. Khakimov, “Geometric imperfection and lower-bound analysis of spherical shells under external pressure,” Thin-Walled Structures, 2019, Vol. 143, No. 106195. [CrossRef]

[15] H. Zhu, D. Liu, H. Bao, Z. Ding, Y. Zhang, “Influence of Initial Imperfections on PMMA Spherical Shell,” Advances in Materials Science and Engineering, 2022, Vol. 2022, No. 3481368. [CrossRef]

[16] S. Pranesh, D. Kumar, V. A. Subramanian, D. Sathianarayanan, G. Ramadass, “Non-linear buckling analysis of imperfect thin spherical pressure hull for manned submersible,” Journal of Ocean Engineering and Science, 2017, Vol. 2, pp. 293–300. [CrossRef]

[17] J. W. Hutchinson, J. M. T. Thompson, “Nonlinear buckling behaviour of spherical shells: barriers and symmetry-breaking dimples,” Philosophical Transactions A, 2017, Vol. 375, No. 20160154. [CrossRef]

[18] X. Gao, S. Park, H. Ma, “Analytical Solution for a Pressurized Thick-Walled Spherical Shell Based on a Simplified Strain Gradient Elasticity Theory,” Mathematics and Mechanics of Solids, 2009, Vol. 14, pp. 747–758. [CrossRef]

[19] L. You, H. Ou, “Steady-State Creep Analysis of Thick-Walled Spherical Pressure Vessels With Varying Creep Properties,” Journal of Pressure Vessel Technology, 2008, Vol. 130, No. 014501. [CrossRef]

[20] K. Karami, M. Abedi, M. Z. Nejad, M. H. Lotfian, “Elastic analysis of heterogeneous thick-walled spherical pressure vessels with parabolic varying properties,” Frontiers of Mechanical Engineering, 2012, Vol. 7, No. 4, pp. 433–438. [CrossRef]

[21] P. Bhaskaran, S. Dharmaraj, R. Sethuraman, R. G. Ananda, “Manufacturing Imperfection Sensitivity Analysis of Spherical Pressure Hull for Manned Submersible,” Marine Technology Society Journal, 2013, Vol. 47, No. 6, pp. 64–72. [CrossRef]

[22] S. B. Pranesh, D. Sathianarayanan, G. A. Ramadass, "Design standards for steel spherical pressure hull for a manned submersible," Journal of Ocean Engineering and Marine Energy, 2022, Vol. 8, pp. 137–151. [CrossRef]

[23] C. Bell, J. Corney, N. Zuelli, D. Savings, "A state of the art review of hydroforming technology: Its applications, research areas, history, and future in manufacturing," International Journal of Material Forming, 2020, Vol. 13, pp. 789–828. [CrossRef]

[24] S. Yuan, X. Fan, "Developments and perspectives on the precision forming processes for ultra-large size integrated components," International Journal of Extreme Manufacturing, 2019, Vol. 1, No. 022002. [CrossRef]

[25] Z. Wang, K. Dai, S. Yuan, Y. Zeng, X. Zhang, "The development of integral hydro-bulge forming (IHBF) process and its numerical simulation," Journal of Materials Processing Technology, 2000, Vol. 102, pp. 168–173. [CrossRef]

[26] Y. Jing, J. Guan, C. Kong, W. Zhao, N. Gomi, X. Zhao, "American Journal of Mechanics and Applications," American Journal of Mechanics and Applications, 2022, Vol. 10, No. 2, pp. 16–24. [CrossRef]

[27] Y. Jing, C. Kong, J. Guan, W. Zhao, A. B. Fukuchi, X. Zhao, "Design and Manufacturing Process of a New Type of Deep-Sea Spherical Pressure Hull Structure," Design, 2023, Vol. 7, No. 12. [CrossRef]

[28] Y. Jing, C. Kong, J. Guan, W. Zhao, X. Zhao, "Integral Hydro-Bulge Forming Method of Spherical Pressure Vessels Using a Triangle Patch Polyhedron," Journal of Pressure Vessel Technology, 2023, Vol. 145, No. 031303. [CrossRef]